Protection for a Wind Turbine Generator in a Large Wind Farm

Tai-Ying Zheng*, Yeon-Hee Kim** and Yong-Cheol Kang†

Abstract – This paper proposes a protection algorithm for a wind turbine generator (WTG) in a large wind farm. To minimize the outage section, a protection relay for a WTG should operate instantaneously for an internal fault or a connected feeder fault, whereas the relay should not operate for an internal fault of another WTG connected to the same feeder or an adjacent feeder fault. In addition, the relay should operate with a delay for an inter-tie fault or a grid fault. An internal fault of another WTG connected to the same feeder or an adjacent feeder fault, where the relay should not operate, is determined based on the magnitude of the positive sequence current. To differentiate an internal fault or a connected feeder fault from an inter-tie fault or a grid fault, the phase angle of the negative sequence current is used to distinguish a fault type. The magnitude of the positive sequence current is then used to decide either instantaneous operation or delayed operation. The performance of the proposed algorithm is verified under various fault conditions with EMTP-RV generated data. The results indicate that the algorithm can successfully distinguish instantaneous operation, delayed operation, or non-operation depending on fault positions and types.

Keywords: Wind turbine generator protection, Outage section minimization, Instantaneous operation, Delayed operation, Non-operation

1. Introduction

In the last decade, wind power generation has become the most promising alternative among the new and renewable energies due to its significant technical advances and viability. Many countries, such as the EU, the US, China, and India, have been very keen on developing as much wind energy as possible and developing a large-size wind farm to reduce its cost and minimize the adverse effect resulting from the fluctuation of wind energy on a grid. Korea intends to construct a large wind farm of 2500 MW in its western offshore by 2019. As its penetration level becomes higher, more reliable operation, control, and protection of a wind farm are necessary.

Several studies on protecting a wind farm have been reported [1−3]. In [1, 2], a source-based protection relay using a shaped directional operating characteristic is proposed. An adaptive distance relay considering the conditions of the wind farm is presented in [3]. These relays are installed at the point of common coupling. If a fault occurs in the wind farm, the whole wind farm will be disconnected.

† Corresponding Author: Dept. of Electrical Engineering, and Wind Energy Grid-Adaptive Technology Research Center and Smart Grid Research Center, Chonbuk National University, Korea. (yckang@jbnu.ac.kr)
* Dept. of Electrical Engineering, and Wind Energy Grid-Adaptive Technology Research Center, Chonbuk National University, Korea. (huanxiong417@hotmail.com)
** Dept. of Electrical Engineering, and Wind Energy Grid-Adaptive Technology Research Center, Chonbuk National University, Korea. (love35021@jbnu.ac.kr)

Methods to protect individual wind turbine generators (WTGs) have also been proposed in [4−5]. These are simply composed of protection elements such as over/under voltage, over/under frequency, and so on. They can successfully protect a WTG when an internal fault occurs. However, these methods cannot distinguish a collector feeder fault, an inter-tie fault, and a grid fault. They also cannot distinguish whether it is a connected feeder fault or an adjacent feeder fault. Thus, the outage section can be wider.

The above mentioned relays may be favorable for a small wind farm but not for a large wind farm. The reason is that the undesirable disconnection of the whole large wind farm has considerable adverse effects on the stability of the grid. Therefore, when a fault occurs in a large wind farm, an outage section should be minimized to attain a reliable operation.

To minimize an outage section, a protection relay for a WTG 1) should operate instantaneously for an internal fault or a connected feeder fault, 2) should not operate for an internal fault of another WTG connected to the same feeder or an adjacent feeder fault, and 3) should operate with a delay for an inter-tie fault or a grid fault.

A protection algorithm for a WTG in a large wind farm is proposed in this paper. An internal fault of another WTG connected to the same feeder or an adjacent feeder fault, where the relay should not operate, is determined based on the magnitude of the positive sequence current. To distinguish an internal fault or a connected feeder fault from an inter-tie fault or a grid fault, the phase angle of the negative sequence current is used to distinguish a fault type.

The magnitude of the positive sequence current is then used to decide on either instantaneous operation or delayed operation. The performance of the proposed algorithm is verified under fault conditions varying the fault types and fault positions with EMTP-RV generated data.

2. Wind Farm Model and Relay Functions

2.1 Configuration of a Wind Farm

Fig. 1 shows a typical wind farm model of 100 MW studied in this paper. Three feeders are connected to a collector bus, which is connected to the grid through the main transformer, substation bus and parallel inter-tie lines. Feeders I and II are connected by two WTGs of 1 MW. WT_{11} and WT_{12} are connected to Feeder I, whereas WT_{21} and WT_{22} are connected to Feeder II. Feeder III contains a large WTG of 96 MW (WT_3), which includes all the other WTGs. All the WTGs are fixed-speed asynchronous squirrel cage induction generators (Type 1).
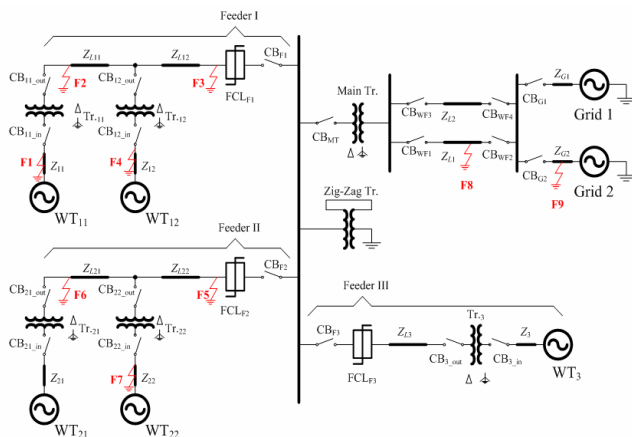

Fig. 1. Wind farm model

In Fig. 1, fault current limiters (FCLs) are installed in each feeder to limit fault current between the end of a feeder and the circuit breaker. The winding connection of a step-up transformer of each WTG is delta-grounded-wye connected. The reason is that this connection isolates the WTGs from the zero sequence behavior of the collector feeder and is a solid ground source for the low voltage side connected to the WTGs [6]. The winding connection of the main transformer is grounded-wye-delta connected. The reason is that some utilities require the connection of a wind farm to be identical to the one typically used for conventional power plants [7]. In the current paper, the ground source of the collector system is provided by a Zig-Zag transformer connected to the collector bus.

2.2 Required WTG Relay Functions

This subsection describes the functions of a WTG (WT_{11}) protection relay in minimizing an outage section when a fault occurs in a wind farm. Table 1 shows the functions a WTG protection relay should have. F1–F9 in Fig. 1 show the fault positions.

Table 1. Required relay functions for WT_{11} to minimize an outage section

Fault positions	Required relay operation
F1–F3	Instantaneous operation
F4–F7	Non-operation
F8, F9	Delayed operation

F1 indicates the internal fault of a WT_{11}, whereas F2 and F3 denote the connected feeder faults. In the cases of F1–F3, the relay for WT_{11} should operate instantaneously.

F4 indicates the internal fault of another WTG (WT_{12}) connected to the same feeder. The relay for WT_{12} should operate instantaneously, whereas the relay for WT_{11} should not operate. F5–F7 denote the adjacent feeder faults, including an internal fault of a WTG connected to an adjacent feeder, where the relay for WT_{11} should not operate.

F8 represents the inter-tie fault. In this case, the WTG relay operation depends on the configuration of the inter-tie, single- or multiple-lines. The relay for WT_{11} for a single-line should operate instantaneously. However, for multiple-lines, the relay should detect the fault and operate with a delay. In the current paper, the configuration of the inter-tie assumes multiple-lines, which is necessary for a modern large wind farm. Thus, the WTG relay should operate with a delay. The delay time should be determined considering the coordination time between the corresponding relays.

F9 indicates the grid fault, which is located far from a WTG. Modern grid codes in many countries require a WTG or a wind farm protection relay to have a low-voltage ride-through (LVRT) capability in this case. Therefore, the WTG relay should be carefully designed to have LVRT capability considering the grid codes of each country. However, this is not the main concern of this paper; thus, it will be discussed in another study.

3. Proposed Algorithm for a WTG

Fig. 2 shows the flowchart of the proposed algorithm. The proposed algorithm is composed of the two stages. At stage 1, the magnitude of the positive sequence current is used to distinguish F4–F7 faults from F1–F3 and F8/F9 faults. At stage 2, the phase angle of the negative sequence current is used to distinguish a fault type. The magnitude of the positive sequence current is then used to decide on either instantaneous operation (F1–F3 faults) or delayed operation (F8/F9 fault).
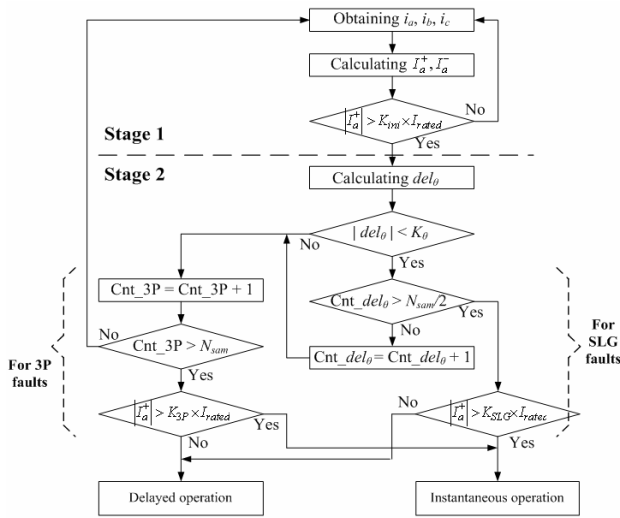
Fig. 2. Flowchart of the proposed algorithm

3.1 Stage 1: Distinguishing F4–F7 from F1–F3 and F8/F9

The magnitude of the positive sequence current is used to distinguish faults at F4–F7 from those at F1–F3 and F8/F9. When a fault occurs at F4–F7, the relay for a WTG connected to the healthy feeder "sees" the fault through its step-up transformer and the FCL installed at the faulted feeder. The equivalent impedance to the fault is so large that the fault current flowing out is limited to a small value, which is almost similar to a normal load current. Hence, the magnitude of the positive sequence current does not increase significantly and is smaller than the threshold (K_{ini}) of a magnitude detector. K_{ini} is decided by fault analysis of the studied system based on symmetrical components. Representing a Type 1 WTG as a voltage source in series with a direct axis sub-transient inductance as well as calculating the maximum fault current using symmetrical components during the first few cycles after a fault are reasonable and convenient [8].

Conversely, the relay for a WTG connected to the faulted feeder "sees" the fault only through its step-up transformer. This is why the magnitude of the positive sequence current increases significantly.

Thus, an internal fault of another WTG connected to the same feeder or an adjacent feeder fault, where the relay should not operate, can be determined successfully based on the magnitude of the positive sequence current.

3.2 Stage 2: Distinguishing F1–F3 from F8/F9

Due to the impedance of the main transformer in the substation, the fault current for the F8/F9 fault is smaller than that of the F1–F3 fault. However, the magnitude of the positive sequence current is not sufficient because the fault current for a three-phase (3P) fault at F8 may be larger than that for a single line-to-ground (SLG) fault at F2 or F3. The

reason is that the negative and zero sequence circuits do not exist in a balanced 3P fault. Thus, the fault type should be determined first.

Using the zero sequence current to determine whether the fault type is SLG or 3P is common. However, in the configuration of Fig. 1, the zero sequence current cannot be used because of its absence due to the connection of the step-up transformer of a WTG.

Thus, in the current paper, the negative sequence current is used to determine the fault type instead of the zero sequence current. The magnitude of the negative sequence current is not used for fault type discrimination because its magnitude is negligible when the fault impedance is high. For an SLG fault, the phase angle (θ) of the negative sequence current remains constant depending on the fault condition, whereas θ does not for a 3P fault due to its absence. Thus, in this paper, θ is used to determine the fault type.

In the current paper, to decide on whether θ is constant, the first difference (del_θ) of θ is used. del_θ is calculated when the magnitude of the positive sequence current exceeds the threshold in Stage 1. If del_θ is smaller than a certain value (K_θ, the threshold of the phase angle detector) for half a cycle, θ is considered a constant, and the fault is considered an SLG fault.

When the fault type has been distinguished, the magnitude of the positive sequence current can be used to distinguish the faults at F1–F3 or F8/F9. Hence, the relay for a WTG can decide an appropriate operation, i.e., delayed operation or instantaneous operation. In this paper, K_{SLG} and K_{3P} are thresholds of the magnitude detectors for an SLG and a 3P fault, respectively. They are also decided using fault analysis of the studied system based on symmetrical components.

4. Case Studies

To verify the performance of the proposed algorithm, a wind farm, as shown in Fig. 1, is modeled using EMTP-RV. Details on the wind farm are mentioned in Section 2. The sampling rate is 64 samples/cycle.

The performance of the algorithm is verified under the various fault conditions by varying the fault positions and fault types, i.e., an SLG fault and a 3P fault.

Case 1: SLG fault at F1

Fig. 3 shows the results for Case 1, where an A-Phase ground fault occurs at WT_{11} at 33.33 ms. The 3P currents (i.e., i_{a_WT11}, i_{b_WT11}, and i_{c_WT11}) measured at the terminal of WT_{11} are shown in Fig. 3(a), where the solid, dashed, and dotted lines represent i_{a_WT11}, i_{b_WT11}, and i_{c_WT11}, respectively. The 3P currents (i.e., i_{a_WT21}, i_{b_WT21}, and i_{c_WT21}) measured at the terminal of WT_{21} are shown in Fig. 3(b). In Fig. 3(c), the solid line shows the magnitude of the positive sequence current ($|I^+_{a\_WT11}|$) calculated from i_{a_WT11},
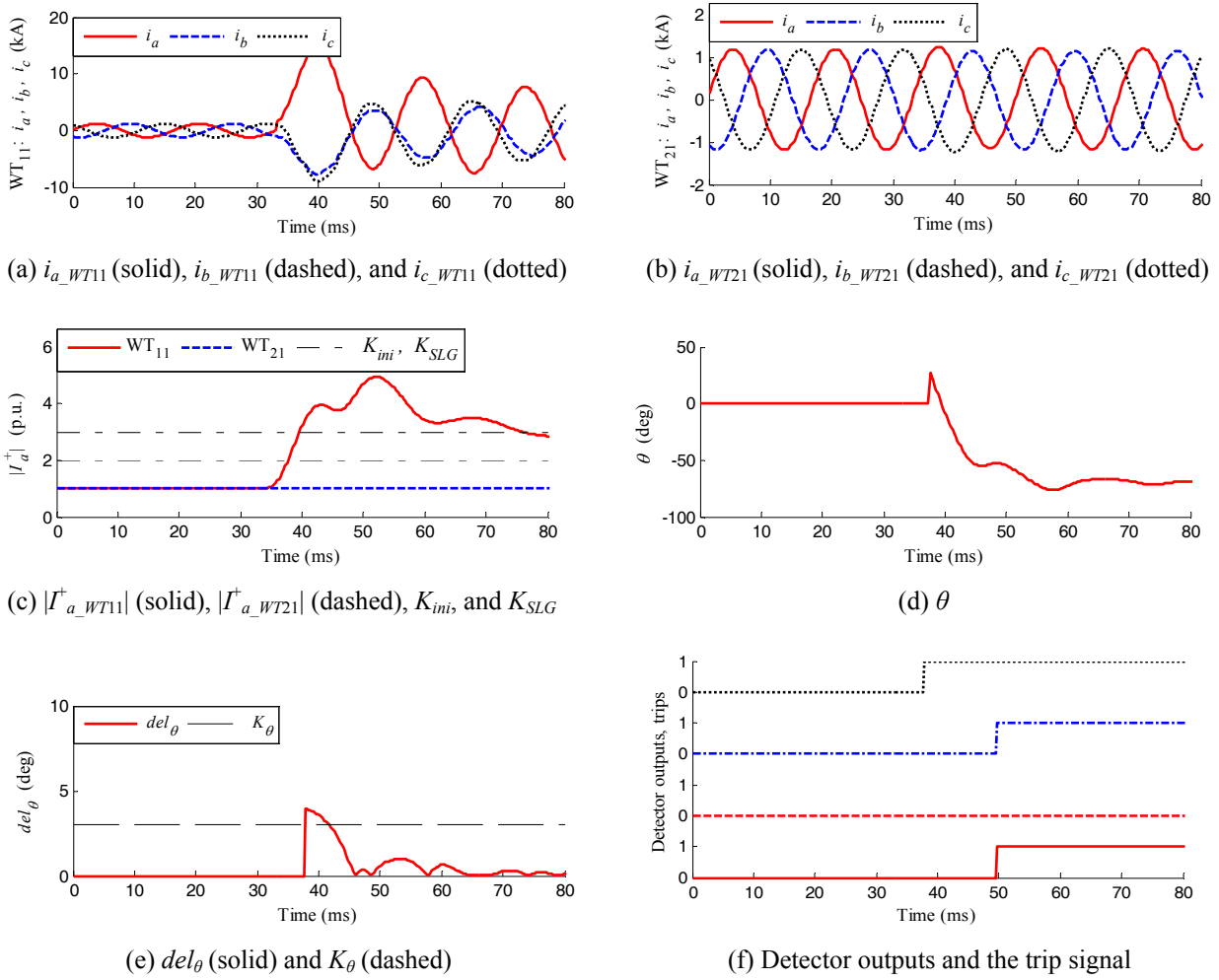
(a) i_{a_WT11} (solid), i_{b_WT11} (dashed), and i_{c_WT11} (dotted)

(b) i_{a_WT21} (solid), i_{b_WT21} (dashed), and i_{c_WT21} (dotted)

(c) $|I^+_{a\_WT11}|$ (solid), $|I^+_{a\_WT21}|$ (dashed), K_{ini}, and K_{SLG}

(d) θ

(e) del_θ (solid) and K_θ (dashed)

(f) Detector outputs and the trip signal

Fig. 3. Results for Case 1

i_{b_WT11}, and i_{c_WT11}, and the dashed line shows ($|I^+_{a\_WT21}|$) calculated from i_{a_WT21}, i_{b_WT21}, and i_{c_WT21}. In the current paper, both $|I^+_{a\_WT11}|$ and $|I^+_{a\_WT21}|$ are shown with per unit quantities. The two dashed-dotted lines show the thresholds of two magnitude detectors, where K_{ini} and K_{SLG} are set to 2 and 3 p.u., respectively.

In this case, because the SLG fault occurs at WT_{11}, $|I^+_{a\_WT11}|$ significantly increases, whereas $|I^+_{a\_WT21}|$ remains the same as before a fault due to the large impedance of an FCL and a step-up transformer. Thus, as mentioned in Section 3, the magnitude of the positive sequence current of WT_{21}, which is connected to an adjacent feeder, increases but not enough to detect a fault. Therefore, the WT_{21} relay does not operate, which means that the proposed WTG protection algorithm does not operate for an adjacent feeder fault.

Fig. 3(d) shows θ calculated from i_{a_WT11}, i_{b_WT11}, and i_{c_WT11}. In this paper, θ is calculated only after the magnitude of the positive sequence current exceeds the threshold value. In Fig. 3(e), del_θ and K_θ are represented by solid and dashed lines, respectively. As described in Section 3, when an SLG fault occurs, θ remains constant,

as seen in Figs. 3(d) and 3(e). Fig. 3(f) shows the magnitude detector output, phase angle detector output, delayed trip signal, and instantaneous trip signal, respectively, from top to bottom. Case 1 is an internal SLG fault, where the relay should operate instantaneously. Thus, the first output signal, which is the output of the magnitude detector in the first stage, is activated at 37.80 ms, when the magnitude of the positive sequence current exceeds the threshold. The second signal, which is the output of the phase angle detector in the second stage, is activated at 49.78 ms because the fault type is an SLG. The fourth "instantaneous trip" signal rather than the third "delayed trip" signal is correctly activated at 49.78 ms because the fault requires the instantaneous trip.

Case 2: 3P fault at F1

Fig. 4 shows the results for Case 2, where a 3P fault occurs at WT_{11} at 33.33 ms. In Fig. 4(a), i_{a_WT11}, i_{b_WT11}, i_{c_WT11}, and $|I^+_{a\_WT11}|$ are larger than those in Case 1. The upper dashed-dotted line in Fig. 4(c) shows K_{3P}, the threshold of the magnitude detector used to distinguish the fault position of a 3P fault. $|I^+_{a\_WT11}|$ exceeds K_{3P}, whereas
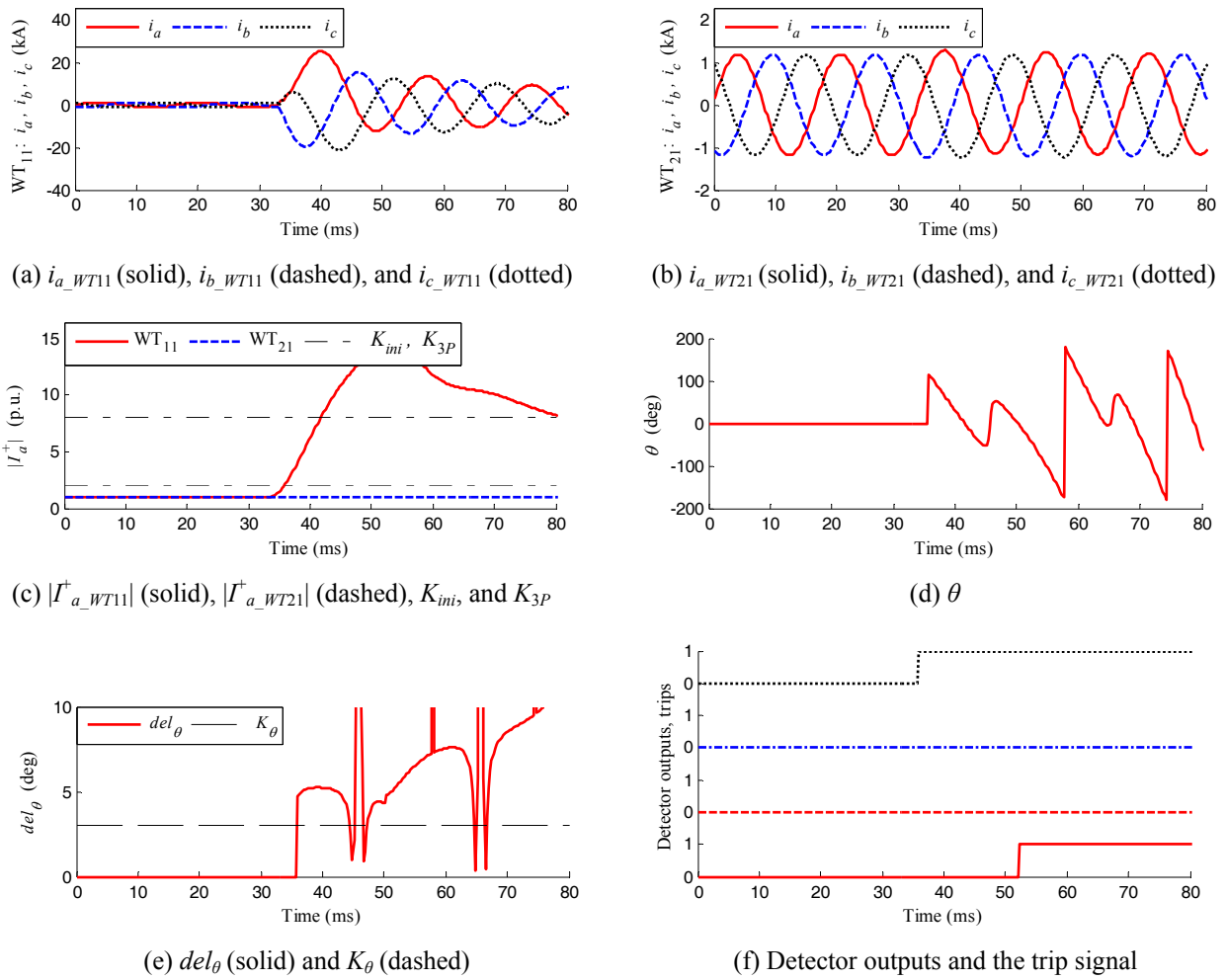
(a) i_{a_WT11} (solid), i_{b_WT11} (dashed), and i_{c_WT11} (dotted)

(b) i_{a_WT21} (solid), i_{b_WT21} (dashed), and i_{c_WT21} (dotted)

(c) $|I^+_{a\_WT11}|$ (solid), $|I^+_{a\_WT21}|$ (dashed), K_{ini}, and K_{3P}

(d) θ

(e) del_θ (solid) and K_θ (dashed)

(f) Detector outputs and the trip signal

Fig. 4. Results for Case 2

$|I^+_{a\_WT21}|$ remains the same as before a fault. As the fault is a balanced fault, and no negative sequence component exists, θ is not a constant and del_θ is larger than K_θ, as shown in Figs. 4(d) and 4(e). This case is an internal 3P fault, where the relay should operate instantaneously. Thus, the activation times of the first output signal, the second output signal, and the final instantaneous trip are activated at 35.98, 52.39, and 52.39 ms, respectively.

The results of Case 1 and 2 indicate that the proposed algorithm can successfully determine whether an internal fault is either an SLG fault or a 3P fault.

Case 3: SLG fault at F3

Fig. 5 shows the results for Case 3. In this case, an A-Phase ground fault occurs at Feeder I at 33.33 ms. Although i_{a_WT11}, i_{b_WT11}, i_{c_WT11}, and $|I^+_{a\_WT11}|$ are smaller than those in Case 1, $|I^+_{a\_WT11}|$ exceeds the threshold of the magnitude detector, as shown in Fig. 5(c). The reason is that the magnitudes of the currents are limited by the impedance of the step-up transformer. However, limited by the impedance of both FCL and step-up transformer, $|I^+_{a\_WT21}|$ does not exceed that threshold. In Fig. 5(f), the

WT$_{11}$ protection relay detects the fault and activates the instantaneous trip signal at 50.04 ms, whereas the WT$_{21}$ protection relay does not operate. The results indicate that the proposed algorithm can distinguish between a connected feeder fault and an adjacent feeder fault.

Case 4: 3P fault at F4

Fig. 6 shows the results for a 3P fault at WT$_{12}$. In Figs. 6(a) and 6(b), i_{a_WT11}, i_{b_WT11}, i_{c_WT11}, i_{a_WT21}, i_{b_WT21}, and i_{c_WT21} are similar to the normal load current. In Fig. 6(c), both $|I^+_{a\_WT11}|$ and $|I^+_{a\_WT21}|$ do not exceed K_{ini}. Thus, θ is not calculated, and neither instantaneous nor delayed trip signals are activated. The results indicate that when an internal fault occurs in another WTG connected to the same feeder, the protection algorithm does not activate the trip signal.
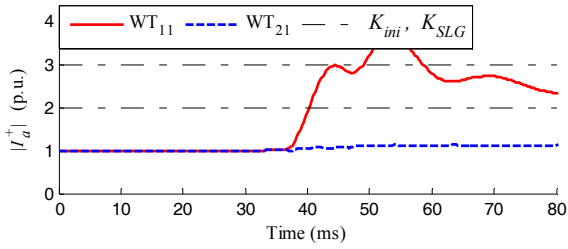
Case 5: SLG fault at F8

Fig. 7 shows the results for Case 5. This is an inter-tie fault, where the relay should operate with a delay. In Figs. 7(a), 7(b), and 7(c), i_{a_WT11}, i_{b_WT11}, i_{c_WT11}, i_{a_WT21}, i_{b_WT21}, and i_{c_WT21} are larger than those prior to the fault, and both
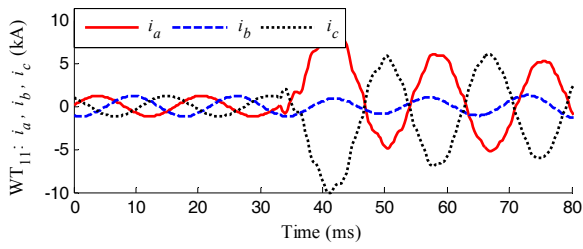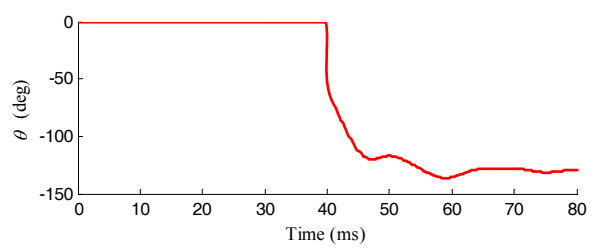
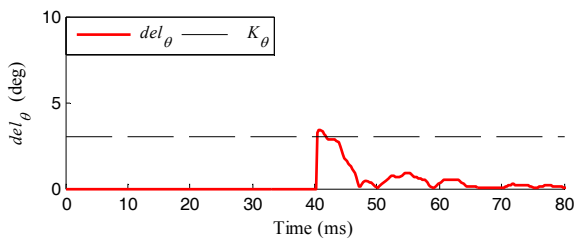(a) i_{a_WT11} (solid), i_{b_WT11} (dashed) and i_{c_WT11} (dotted)
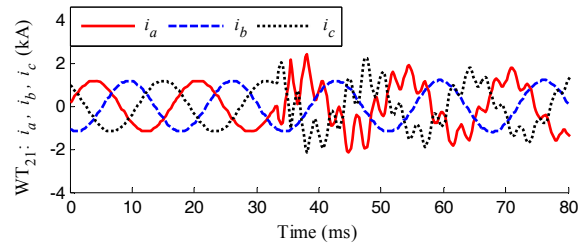
(b) i_{a_WT21} (solid), i_{b_WT21} (dashed), and i_{c_WT21} (dotted)
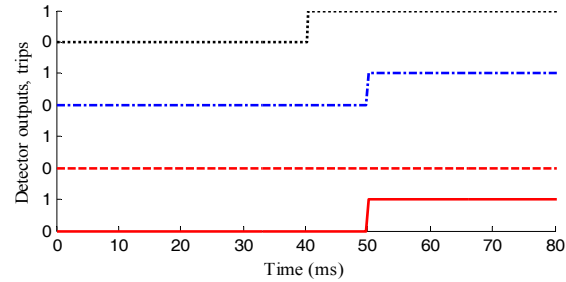
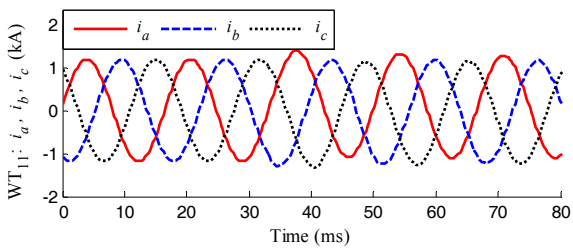(c) $|I^+_{a\_WT11}|$ (solid), $|I^+_{a\_WT21}|$ (dashed), K_{ini}, and K_{SLG}

(d) θ

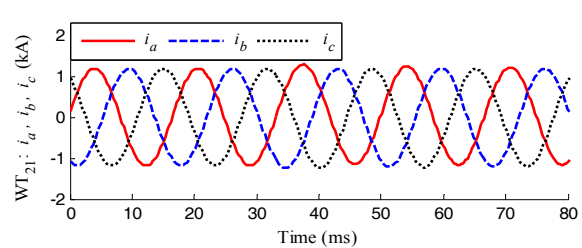(e) del_θ (solid) and K_θ (dashed)

(f) Detector outputs and the trip signal

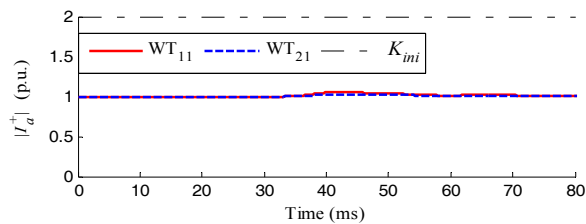**Fig. 5.** Results for Case 3

(a) i_{a_WT11} (solid), i_{b_WT11} (dashed), and i_{c_WT11} (dotted)

(b) i_{a_WT21} (solid), i_{b_WT21} (dashed), and i_{c_WT21} (dotted)

(c) $|I^+_{a\_WT11}|$ (solid), $|I^+_{a\_WT21}|$ (dashed), and K_{ini}

Fig. 6. Results for Case 4

(a) i_{a_WT11} (solid), i_{b_WT11} (dashed), and i_{c_WT11} (dotted)

(b) i_{a_WT21} (solid), i_{b_WT21} (dashed), and i_{c_WT21} (dotted)

(c) $|I^+_{a\_WT11}|$ (solid), $|I^+_{a\_WT21}|$ (dashed), K_{ini}, and K_{SLG}

(d) θ

(e) del_θ (solid) and K_θ (dashed)

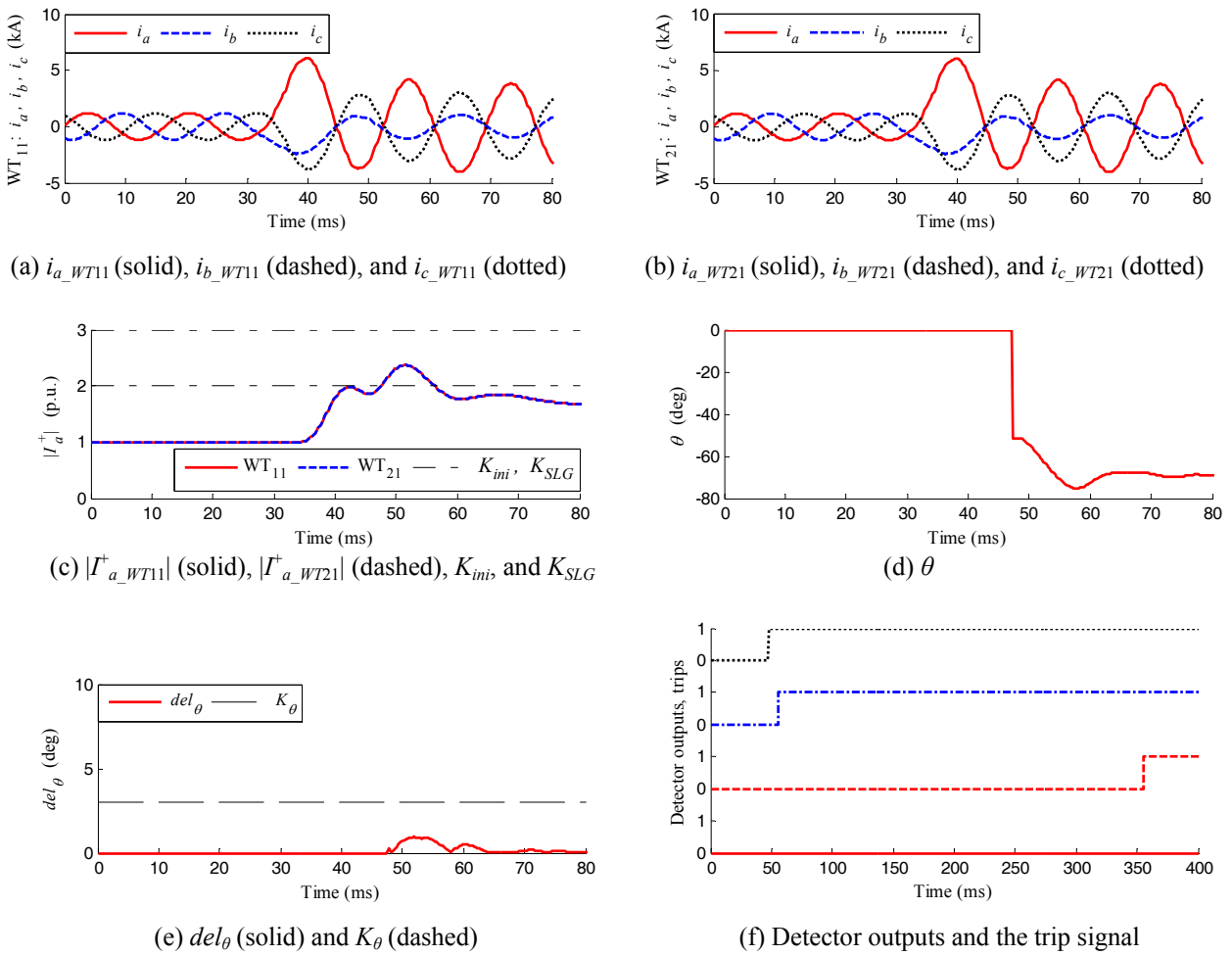(f) Detector outputs and the trip signal

Fig. 7. Results for Case 5

$|I^+_{a\_WT11}|$ and $|I^+_{a\_WT21}|$ exceed K_{ini}. However, due to the impedance of the main transformer in the substation, these cannot exceed K_{SLG}, as seen in Fig. 7(c). In Fig. 7(f), the first and second output signals are activated at 47.70 and 55.77 ms, respectively. The delayed operation signal is activated at 55.77 ms. Finally, the delayed trip signal is activated at 355.77 ms. In the current paper, the coordination time is set to 300 ms, which is commonly used in distribution system protection. The results indicate that when an inter-tie fault occurs, a delayed operation signal rather than an instantaneous operation signal is activated successfully.

5. Conclusion

This paper proposes a protection algorithm for a WTG in a large wind farm to minimize the outage section. The magnitude of the positive sequence current is used to determine an internal fault of another WTG connected to the same feeder or an adjacent feeder fault. To differentiate an internal fault or a connected feeder fault from an inter-tie fault or a grid fault, the phase angle of the negative sequence current is used to distinguish a fault type. The magnitude of the positive sequence current is then used to decide on either instantaneous operation or delayed operation.

The simulation results clearly indicate that the proposed WTG protection algorithm can successfully distinguish instantaneous, delayed, or non-operation depending on fault positions and types.

The proposed algorithm can minimize the outage section, preventing the undesirable disconnection of an entire large wind farm or some healthy WTGs.

Acknowledgments

References

[1] S. J. Haslam, P. A. Crossley, and N. Jenkins, "Design and field testing of a source based protection relay for wind farms," *IEEE Trans. on Power Deliv.*, Vol. 14, No. 3, pp. 818–823, Jul. 1999.

[2] S. J. Haslam, P. A. Crossley, and N. Jenkins, "Design and evaluation of a wind farm protection relay," *IEE Proc. -Gener. Transm. Distrib.*, Vol. 146, No. 1, pp. 37–44, Jan. 1999.

[3] A. K. Pradhan, and Géza Joós, "Adaptive distance relay setting for lines connecting wind farms," *IEEE Trans. on Energy Conversion*, Vol. 22, No. 1, pp. 206–213, Mar. 2007.

[4] GE Consumer & Industrial Multilin, W650-Wind generator protection system instruction manuals, 2006 GE Multilin. [online]. Available: http://www.gedigitalenergy.com/app/ViewFiles.aspx?prod=w650&type=3

[5] Schweitzer Engineering Laboratories, SEL-700GW wind generator relay. [online]. Available: http://www.selinc.com/sel-700gw/

[6] Wind Plant Collector Design WG, "Wind power plant grounding, overvoltage protection, and insulation coordination," in *Proc. 2009 IEEE Power and Energy Society General Meeting*, Calgary, Canada, Jul. 2009.

[7] Wind Plant Collector Design WG, "Wind power plant substation and collector system redundancy, reliability, and economics," in *Proc. 2009 IEEE Power and Energy Society General Meeting*, Calgary, Canada, Jul. 2009.

[8] N. Samman, R. Zavadil, J. C. Smith, and J. Conto, "Modeling of wind power plants for short circuit analysis in the transmission network," in *Proc. Of IEEE/PES Transmission and Distribution Conference*, Chicago, USA, Apr. 2008.

Tai-Ying Zheng He received his B. S. and M. S. degrees from Zhe Jiang University, Hang Zhou, China, in 2004, and Chonbuk National University, Chonju, Korea, in 2006, respectively. He is currently pursuing his Ph.D. degree in Chonbuk National University, Chonju, Korea. His research interest is the development of new protection and control systems for a wind farm.

Yeon-Hee Kim He received his B.S. and M.S. degrees from Chonbuk National University, Korea, in 2006 and 2008, respectively. He is currently taking his Ph.D. degree in Chonbuk National University. His research interest is the development of new protection systems for power systems using digital signal processing techniques.

Yong-Cheol Kang He received his B.S., M.S., and Ph.D. degrees from Seoul National University, Korea, in 1991, 1993, and 1997, respectively. He has been with Chonbuk National University, Korea, since 1999. He is currently a professor in Chonbuk National University, Korea, and the director of the wind energy grid-adaptive technology center supported by the Ministry of Education, Science, and Technology, Korea. He is also with Smart Grid Research Center in Chonbuk National University. His research interest is the development of new protection and control systems for a wind farm.